Available online at www.sciencedirect.com
ScienceDirect
Journal of the European Ceramic Society 27 (2007) 2077–2083
www.elsevier.com/locate/jeurceramsoc

Influence of silicon carbide particle size on the microstructure and mechanical properties of zirconium diboride–silicon carbide ceramics

Sumin Zhu *, William G. Fahrenholtz, Gregory E. Hilmas

Department of Materials Science and Engineering, University of Missouri-Rolla, Rolla, MO 65409, USA

Received 19 May 2006; received in revised form 5 July 2006; accepted 15 July 2006
Available online 7 September 2006

Abstract

The influence of silicon carbide (SiC) particle size on the microstructure and mechanical properties of zirconium diboride–silicon carbide (ZrB_2–SiC) ceramics was investigated. ZrB_2-based ceramics containing 30 vol.% SiC particles were prepared from four different α-SiC precursor powders with average particle sizes ranging from 0.45 to 10 μm. Examination of the dense ceramics showed that smaller starting SiC particle sizes led to improved densification, finer grain sizes, and higher strength. For example, ceramics prepared from SiC with the particle size of 10 μm had a strength of 389 MPa, but the strength increased to 909 MPa for ceramics prepared from SiC with a starting particle size of 0.45 μm. Analysis indicates that SiC particle size controls the strength of ZrB_2–SiC.

Keywords: Borides; SiC; Composites; Microstructure; Mechanical properties

1. Introduction

Ultra-high temperature ceramics (UHTCs) include borides, carbides, and nitrides with melting temperatures above ~2700 °C.[1] The UHTCs have been investigated for high temperature applications including thermal protection systems for hypersonic aerospace vehicles, high temperature electrodes, and molten metal crucibles.[2–5] Recently, zirconium diboride (ZrB_2) based ceramics have been studied because of their unique combination of low density, high melting temperature and thermal shock resistance as well as excellent mechanical and chemical stability at high temperatures.[6–9]

ZrB_2–SiC ceramics, of suitable composition, are known to have better strength and oxidation resistance than monolithic ZrB_2.[10,11] A recent study of several ZrB_2-based ceramics demonstrated that ZrB_2 with 30 vol.% SiC addition exhibited the best combination of strength, fracture toughness, and oxidation resistance.[12] The addition of SiC particles enhances the oxidation resistance of ZrB_2 by promoting the formation of a protective borosilicate glass layer.[13] High strength has been attributed to maintaining a fine grain size and a uniform distribution of the reinforcing phase.[11] Monteverde and Bellosi reported that incorporation of ultra-fine SiC improved the sinterability and mechanical properties of ZrB_2.[14,15] Subsequently, Rezaie et al. proposed that the strength limiting flaws in ZrB_2–SiC were the largest SiC particles observed in the microstructure.[16] Based on the combined evidence, it can be concluded that the size of the SiC particles plays a critical role in determining the microstructure and mechanical properties of ZrB_2–SiC composites.

In this paper the microstructure and mechanical properties of hot pressed ZrB_2–SiC ceramics, prepared from a single grade of ZrB_2 powder, and four different SiC precursor powders, were studied. The sintered density, microstructure, and mechanical properties were evaluated and compared.

2. Experimental procedure

2.1. Materials and processing

Commercial ZrB_2 and SiC powders were used in this study. Table 1 lists the characteristics of the powders based on data from the suppliers. All four SiC powders were predominantly α-SiC. Prior to hot pressing, the as-received ZrB_2 was batched with one of the SiC powders in a 70:30 volume ratio (82:18 weight ratio) into a fluoropolymer-coated tank for attrition milling (Model 01-HD, Union Process, Akron, OH). The

* Corresponding author.
E-mail address: smzhu2005@hotmail.com (S. Zhu).

0955-2219/$ – see front matter © 2006 Elsevier Ltd. All rights reserved.
doi:10.1016/j.jeurceramsoc.2006.07.003

Table 1
Characteristics of raw materials

Material	Grade	Mean particle size (μm)	Specific surface area (m^2/g)	Purity (%)	Supplier
ZrB_2	A	6	1	>99	H.C. Starck
SiC	600 grit	~10	0.4	99.5	Universal Photonics
SiC	UF05	1.4	5	98.5	H.C. Starck
SiC	UF10	0.7	10	98.5	H.C. Starck
SiC	UF25	0.45	25	98.5	H.C. Starck

powders were milled in hexane at 600 rounds per minute (rpm) for 2 h, using Co-bonded WC media and a Co-bonded WC spindle. For the 600 grit SiC, the powder was added into the milling tank for only the last 15 min to minimize particle size reduction, but still provide adequate mixing. All of the powder mixtures were dried by rotary evaporation (Model Rotavapor R-124, Buchi, Flawil, Germany) at a temperature of 75 °C, a vacuum of 30 kPa, and a rotation speed of 150 rpm. Powder mixtures were designated by the letters ZS (for ZrB_2 and SiC) along with the initial size of the SiC precursor powder. For example, the material prepared from ZrB_2 and 1.4 μm SiC was designated ZS1.4.

The powder mixtures were hot pressed (Model HP-3060, Thermal Technology, Santa Rosa, CA) in a 44-mm-diameter graphite die lined with BN coated graphite foil. The temperature of the graphite die was monitored with an infrared pyrometer (Model OS 3708, Omega Engineering, Stamford, CT). At temperatures below 1650 °C, the furnace was heated under ~20 Pa vacuum. Above 1650 °C, the atmosphere was switched to flowing argon gas. A heating rate of ~20 °C/min was used between room temperature and 1900 °C. When the furnace reached a temperature of 1900 °C, a uniaxial pressure of 32 MPa was applied. The furnace was held at this temperature for 45 min. At the end of the hold, the furnace was cooled at a rate of ~20 °C/min. The load was removed at ~1750 °C.

2.2. Characterization

The specific surface areas of the powder mixtures after attrition milling were characterized using nitrogen adsorption (NOVA 1000, Quantachrome, Boynton Beach, FL) at 77 K and BET (Brunnauer–Emmett–Teller) analysis. The particle sizes of the milled powders and grain sizes of the densified ceramics were determined from scanning electron microscopy images (SEM; Model S4700 Hitachi, Tokyo, Japan) using an image analysis software package (ImageJ, National Institute of Health, Bethesda, MD). A minimum of 100 measurements were performed for each average value reported. The bulk density of each hot pressed specimen was measured using the Archimedes' method with water as the immersing medium. Specimens were saturated by boiling for 2 h and then cooling to room temperature. The true density of each composition was measured using helium pycnometry (Model 1305 Multivolume, Micromeritics Instrument Corp., Norcross, GA) on hot pressed materials that were ground to −200 mesh (~77 μm) to expose as much of the closed porosity as possible. The amount of WC incorporated into each batch was estimated by comparing the measured true density with the density predicted from the nominal ZrB_2 to SiC ratio (5.2 g/cm^3 for ZrB_2 + 30 vol.% SiC). The microstructure of the hot pressed specimens was investigated by examining fracture surfaces and polished cross-sections in the SEM. Vickers' microhardness measurements (Model V-1000-A2, Leco, St. Joseph, MI) were performed at a test load of 0.2 kg (~2 N) and a dwell time of 20 s. The low test load was used due to cracking problems at higher test loads in some specimens. An average of 10–12 indentations were taken for each reported value. Young's modulus (E) and Poisson's ratio (ν) were measured on 44-mm diameter disc-shaped specimens by impulse excitation of vibration (Model MK4-I Grindosonic, J.W. Lemmens, St. Louis, MO) according to ASTM standard C1259-01. The fracture toughness was determined by fracturing specimens after indentation according to the indentation strength in bending method described by Chantikul et al.[17] A load of 10 kg was used to produce radial-median cracks before fracturing the specimens in four point bending. The equation used for calculating fracture toughness, K_{Ic}, was

$$K_{Ic} = 0.59\left(\frac{E}{H}\right)^{1/8}(\sigma_m P^{1/3})^{3/4} \quad (1)$$

where E is Young's modulus, H the Vickers' microhardness, σ_m the measured four-point bend strength after indentation, and P is the indentation load. The fracture toughness data were based on an average of five measurements for each composition. The four-point bend strength was measured according to ASTM standard C1161-02a. Type A specimens (dimensions of 1.5 mm × 2 mm × 25 mm) were fractured in four-point bending using inner and outer spans of 10 and 20 mm, respectively, and a crosshead speed of 0.2 mm/min. Ten measurements were conducted for each material to calculate the average strength and the corresponding standard deviations.

3. Results and discussion

3.1. Powder characterization

The average particle sizes of both ZrB_2 and SiC powders decreased substantially during milling (Fig. 1). For example, the average particle size of SiC decreased from 1.4 to 1.1 μm, and that of ZrB_2 from 6.0 to 0.6 μm after milling the ZS1.4 material. SEM analysis revealed no SiC particles larger than 2 μm in the milled powder mixture of the ZS0.45 material (Fig. 1d). However, some residual SiC particles larger than 2 μm were observed in the other powder mixtures (Fig. 1a–c). The BET analysis results confirmed the difference in particle size of the attrition milled powder mixtures. The specific surface area of powder

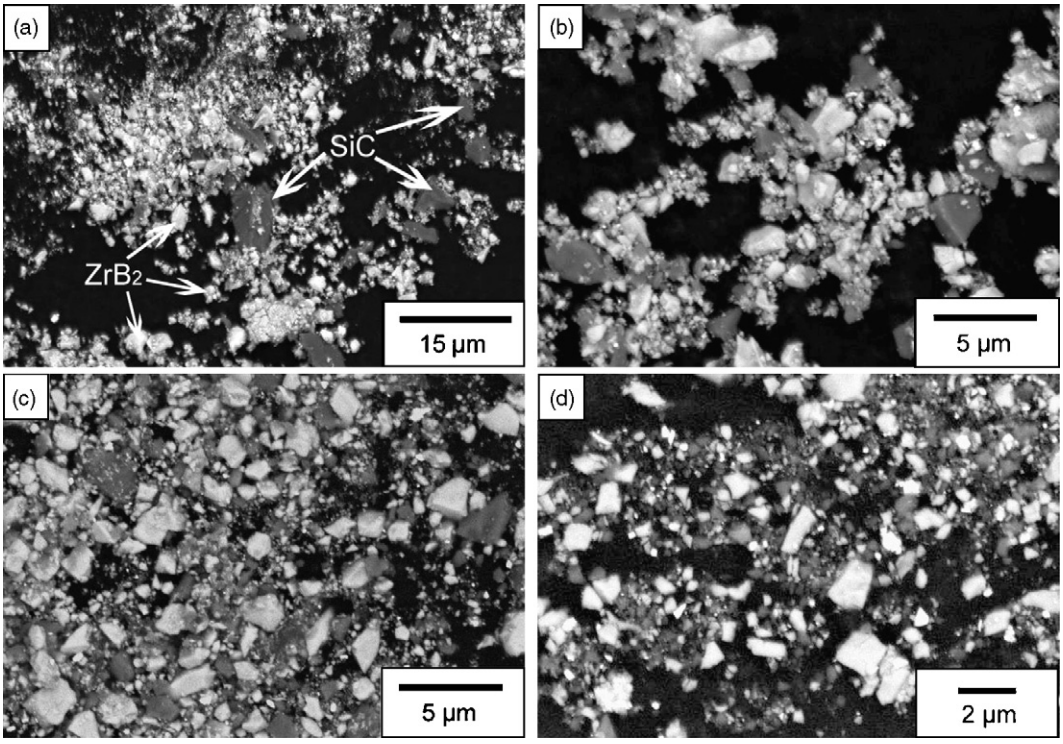

Fig. 1. Morphologies of the attrition milled powder mixtures: (a) ZS10; (b) ZS1.4; (c) ZS0.7; (d) ZS0.45. In these images ZrB_2 is brighter and SiC is darker. Note that the magnification varies among the images.

mixture ZS0.45 was 10.46 m^2/g, but it was only 4.68 m^2/g for powder mixture ZS10. The specific surface areas of powder mixtures ZS1.4 (6.90 m^2/g) and ZS0.7 (6.94 m^2/g) were approximately the same, even though the starting SiC powders had different average particle sizes. To maintain as large of a particle size as possible, the 10 μm SiC powder was added near the end of the milling process to retain larger SiC particles and to avoid the chance of reducing its particle size to the same level as the other batches.

3.2. Density and microstructure

Each of the powder batches picked up a certain amount of WC during milling due to wear of the milling media and spindle. Because the Co-bonded WC used for the media and spindle had a significantly higher density (14.9 g/cm^3) than the ZrB_2 (6.1 g/cm^3) and SiC (3.2 g/cm^3), its presence increased the true density of the resulting powder mixtures. The bulk density determined by Archimedes' method, the measured true density, the relative density of the hot pressed billet, and the estimated WC contents are summarized in Table 2. The WC content was shown to increase from 1.88 to 3.82 vol.% as the size of the SiC precursor powder decreased. Presumably, the increase in WC content with the decrease in starting SiC particle size is related to the efficiency of the milling process, which should decrease as the average particle size decreases. The presence of WC has been reported to have beneficial effects on both the densification and strengthening of ZrB_2-based ceramics, but the mechanisms have not been fully investigated.[9,11,18]

All of the specimens exhibited a high relative density after hot pressing. The relative density of ZS0.45 reached 99.8%. The other materials had slightly lower relative densities, but all were greater than 97.4%. The finer SiC powders appeared to have a beneficial effect on the densification of ZrB_2–SiC ceramics since relative density increased as starting particle size decreased.

The microstructures of the hot pressed composites are shown in Fig. 2, and the measured grain sizes are summarized in Table 3. Some porosity was observed in the hot pressed ZS10 material (Fig. 2a), which is consistent with the lower relative density measured for this material, which was 97.4%. The average grain sizes of both ZrB_2 (3.0 μm) and SiC (6.3 μm) of the ZS10 material were much larger than those of materials

Table 2
Density and WC content of hot pressed ZrB_2–30 vol.% SiC samples

Particle size of SiC precursor (μm)	Material designation	Archimedes density (g/cm^3)	True density (g/cm^3)	Relative density (%)	WC content (vol.%)
~10	ZS10	5.26	5.40	97.4	1.88
1.4	ZS1.4	5.37	5.43	98.9	2.20
0.7	ZS0.7	5.41	5.48	98.7	2.74
0.45	ZS0.45	5.57	5.58	99.8	3.82

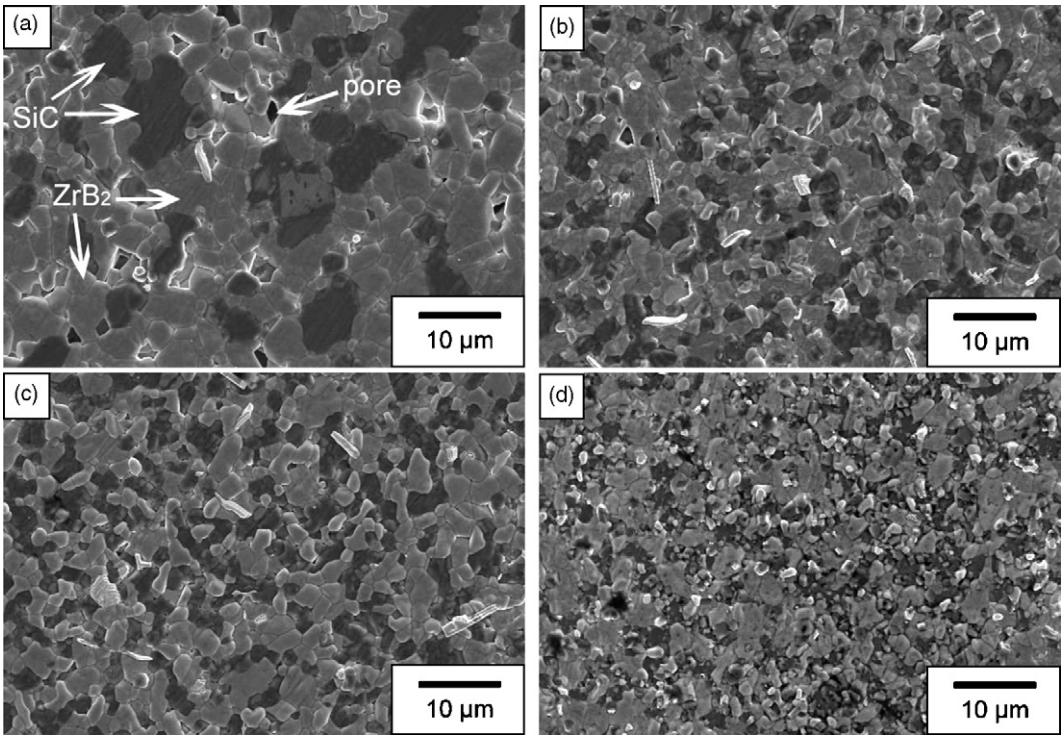

Fig. 2. Microstructure of ZrB_2–SiC hot pressed from: (a) ZS10; (b) ZS1.4; (c) ZS0.7; (d) ZS0.45. In these images ZrB_2 is gray and SiC is black.

prepared from the finer starting SiC powders. By comparison, Fig. 2d shows that the ZS0.45 specimen had little porosity (>99% dense), and it had the finest average grain sizes of ZrB_2 (1.2 μm) and SiC (1.0 μm). Analysis by SEM confirmed that the density of the specimens prepared from finer SiC starting particles were hot pressed to higher relative density than materials prepared from larger particles. In addition, the use of finer starting particles led to finer ZrB_2 and SiC grain sizes in the final ceramics.

Although the starting ZrB_2 powder was the same for all of the specimens in the present study, the average particle size of the starting SiC powder played an important role in controlling the final microstructure of the hot pressed composites, including controlling the ZrB_2 grain size. As shown in Table 3, the average and maximum grain sizes of ZrB_2 are dependent on the size of the starting SiC particles, and this means that smaller starting SiC particles can be used to produce finer microstructures in hot pressed ZrB_2–SiC ceramics. Previous research has revealed that SiC particles acted as grain-growth inhibitors in ZrB_2 and TiB_2 ceramics.[11,19] The results of this study indicate that finer, well dispersed SiC particles are more effective at pinning grain growth in ZrB_2–SiC than larger SiC particles.

3.3. Mechanical properties

Young's modulus, Poisson's ratio, Vickers' microhardness, and fracture toughness were measured for all of the specimens (Tables 4 and 5). The Young's modulus appeared to increase as the starting SiC particle size decreased. However, as discussed above, the density of the hot pressed materials showed a small, but measurable increase as the starting SiC particle size decreased. Therefore, the effect of porosity on the Young's modulus must also be considered. The relationship between porosity and Young's modulus proposed by Nielsen is[20]:

$$E = E_0 \frac{(1-P)^2}{1+(1/\rho-1)P} \quad (2)$$

where E is the modulus of specimens at a porosity P, E_0 the modulus without porosity, and ρ is the Neilsen shape factor (0.4). Using the measured porosity of 0.2% for ZS0.45 (99.8% dense) and a measured modulus of 520 GPa, E_0, the modulus of the fully dense material, would be 524 GPa according to Eq. (2). Further, Nielsen's relationship can be used to predict modulus values as a function of porosity. For example, a modulus of 478 GPa was calculated for ZrB_2–SiC with 2.6% porosity. The calculated

Table 3
Measured grain sizes of the ZrB_2–SiC materials

Material	Average ZrB_2 grain size (μm)	Maximum ZrB_2 grain size (μm)	Average SiC grain size (μm)	Maximum SiC grain size (μm)
ZS10	3.0 ± 1.3	6.8	6.3 ± 2.9	14.5
ZS1.4	1.7 ± 0.7	3.9	2.1 ± 0.7	4.0
ZS0.7	1.6 ± 0.6	3.8	1.6 ± 0.7	3.6
ZS0.45	1.2 ± 0.4	2.5	1.0 ± 0.4	1.9

Table 4
Young's modulus (E) as a function of porosity for ZrB_2–SiC ceramics

Material	Relative density (%)	Porosity (%)	Measured E (GPa)	Calculated E (GPa)
ZS10	97.4	2.6	479 ± 5	478
ZS1.4	98.9	1.1	509 ± 3	504
ZS0.7	98.7	1.3	515 ± 7	501
ZS0.45	99.8	0.2	520 ± 7	520
ZrB_2–SiC	100	0.0	–	524

result is in excellent agreement with the value of 479 GPa measured experimentally for the ZS10 (97.4% dense). In fact, the measured moduli agree with the trend predicted using Nielsen's relationship and the measured density values as summarized in Table 4. The conclusion that can be drawn is that elastic modulus was not affected by the size of the ZrB_2 or SiC particles, as expected for an inherent material property. Similarly, Poisson's ratio did not vary significantly for any of the specimens (Table 5).

The Vickers' microhardness data are summarized in Table 5. The ZS0.45 material had the highest value at 20.7 GPa, and the ZS10 material had the lowest microhardness of 17.5 GPa. The microhardness decreased as the initial SiC particle size increased. Both grain size and relative density could affect the microhardness. Part of the increase in microhardness observed for a decreasing SiC particle size could be explained through a grain size effect. As shown in Table 3, the grain sizes of both SiC and ZrB_2 decreased as the starting particle size of the SiC powder decreased. Smaller grain sizes increase the frequency with which dislocations encounter grain boundaries, thus requiring larger stresses for deformation to occur.[21] In addition to the effect of grain size, relative density also influences microhardness. The pores in ceramics have no resistance to applied stress, so materials with more porosity have lower apparent microhardness values than the dense counterparts. Given that the materials prepared for this study showed a decrease in grain size and an increase in density as the size of starting SiC particles decreased, the trend observed in the microhardness measurements appears to be reasonable.

The fracture toughness values for the four different ZrB_2–SiC composites ranged from ~4.2 to ~4.6 MPa $m^{1/2}$ (Table 5). Considering the standard deviation of the data, the results were statistically identical to each other. However, the fracture toughness for the ZrB_2–SiC composites is substantially higher than that of the monolithic ZrB_2, which is reported to be ~3.5 MPa $m^{1/2}$.[11] A probable explanation is the presence of SiC grains in the microstructure of the composites. Fig. 3 is a SEM image of a crack path on the polished surface of a ZS0.45 material, showing

Table 5
Poisson's ratio (ν), Vickers microhardness (HV0.2), fracture toughness (K_{Ic}), and four-point bend strength (σ) for ZrB_2–SiC

Material	ν	HV0.2 (GPa)	K_{Ic} (MPa $m^{1/2}$)	σ (MPa)
ZS10	0.16	17.5 ± 0.4	4.5 ± 0.1	389 ± 45
ZS1.4	0.15	19.1 ± 1.0	4.3 ± 0.3	805 ± 71
ZS0.7	0.15	19.3 ± 0.6	4.2 ± 0.2	837 ± 116
ZS0.45	0.16	20.7 ± 1.0	4.6 ± 0.1	909 ± 136

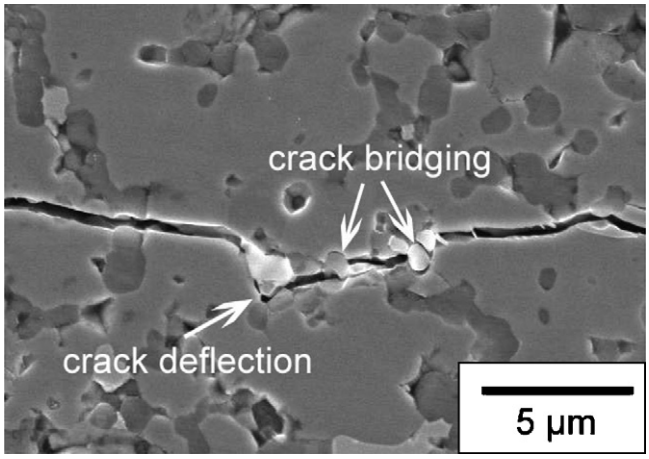

Fig. 3. SEM image showing possible crack deflection and crack bridging near SiC particles in the ZS0.45 material.

possible crack deflection and crack bridging near SiC particles. These mechanisms cause energy dissipation during the fracture of ceramics and have been associated with enhanced fracture toughness.[22,23]

Four-point bend strengths are shown in Table 5 and Fig. 4. The strength increased as the starting SiC particle size decreased. The strength was 389 MPa for the ZS10 material, but increased to a value of 909 MPa for ZS0.45. The strength values for ZS1.4 and ZS0.7 materials were found to be 805 and 837 MPa, respectively. Strength increased significantly as the size of the SiC precursor powders decreased. In Fig. 4, the strength values are plotted as

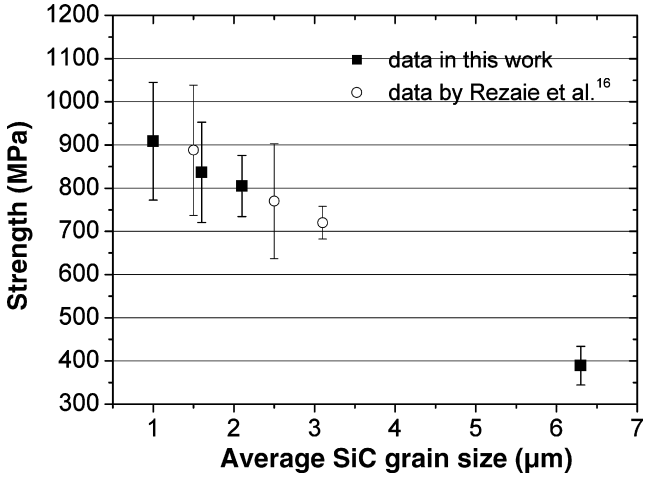

Fig. 4. Four-point bend strength of the hot pressed ZrB_2–SiC as a function of the SiC grain size.

Table 6
Comparison between the strength (σ) ratios and grain size ratios for hot pressed samples

Ratio relation	Strength (σ) ratio	$1/\sqrt{c}$ ratio			
		Average ZrB_2 grain size	Maximum ZrB_2 grain size	Average SiC grain size	Maximum SiC grain size
ZS1.4/ZS10	2.07	1.33	1.32	1.73	1.90
ZS0.7/ZS10	2.15	1.37	1.34	1.98	2.01
ZS0.45/ZS10	2.34	1.58	1.65	2.51	2.76

a function of the average SiC grain size and compared to values obtained by Rezaie et al.[16] The present results support the earlier results that the SiC grain size controls the strength of ZrB_2–SiC ceramics. This work not only verifies the earlier results, but also extends them to higher (>6 μm) and lower (∼1 μm) SiC grain sizes. However, this comparison does not directly relate strength to ZrB_2 or SiC grain sizes, which requires more detailed analysis.

Fracture strength of brittle materials is a function of the critical flaw size as described by the Griffith equation[24]:

$$\sigma_{\text{fracture}} = \frac{K_{\text{Ic}}}{Y\sqrt{c}} \tag{3}$$

where σ_{fracture} is the fracture strength, K_{Ic} the fracture toughness, Y a constant related to the fracture origin, and c is the critical flaw size in the material. As discussed above, fracture toughness values for the four ZrB_2–SiC materials in the present study are statistically identical to each other. Assuming that Y is also a constant for all the specimens, the strength is then inversely proportional to the square root of the critical flaw size, and the following relation can be derived:

$$\sigma_{\text{fracture}} \propto \frac{1}{\sqrt{c}} \tag{4}$$

Based on the SEM observations of as-polished and fractured surfaces of at least five bend bars, no macroscopic flaws were identified as probable fracture origins. In cases, where no other larger defects can be identified, the critical flaw size is often taken as the characteristic grain size.[25] The measured grain sizes for all the four materials are summarized in Table 3. The ZS10 material had the lowest strength and the largest average grain sizes of SiC (6.3 μm) and ZrB_2 (3.0 μm). As shown in Table 3, the ZS1.4 and ZS0.7 materials had similar SiC (2.1 and 1.6 μm) and ZrB_2 (1.7 and 1.6 μm) grain sizes, and exhibit similar strength values (805 and 837 MPa). The ZS0.45 material had the highest strength (909 MPa), which can be attributed to the fact that it had the smallest average grain sizes for both ZrB_2 (1.2 μm) and SiC (1.0 μm).

To correlate strength and grain size, the ratios of strengths and grain sizes among different materials were calculated (Table 6). From the calculated results, both the average and maximum grain sizes of SiC are shown to have better correlations with strength values than the average and maximum ZrB_2 grain sizes. The conclusion that can be drawn from these results is that the SiC grain size (average, maximum, or both) has a much stronger influence on the strength of ZrB_2–SiC than ZrB_2 grain size despite the fact that ZrB_2 is the major phase.

4. Conclusion

The effect of the starting SiC particle size on the microstructure and mechanical properties of hot pressed ZrB_2–SiC ceramics was investigated. Decreasing the average size of starting SiC particles enhanced the densification of ZrB_2–SiC, producing relative densities that increased from 97.4 to 99.8%, as the size of the SiC particles decreased from 10 to 0.45 μm. Analysis by SEM revealed that both the ZrB_2 and SiC grain sizes in dense, hot pressed ceramics decreased as the size of the SiC decreased, indicating that finer SiC particles may be more effective at pinning grain growth during densification. The Young's modulus value was sensitive to the porosity of the ceramics, but showed no direct relationship with the grain size. Vickers microhardness increased from 17.5 GPa for the ZS10 material to 20.7 GPa for the ZS0.45 counterpart. Four-point bend strength was a strong function of SiC grain size, increasing from ∼400 MPa when the average SiC grain size was ∼6 μm to over 900 MPa when the average SiC grain size was ∼1 μm. Based on this research, it can be concluded that the SiC grain size has a strong influence on the strength of ZrB_2–SiC ceramics for average SiC grain sizes ranging from 1 to 6 μm.

Acknowledgements

This work was supported by the National Science Foundation on Grant DMR-03-46800. The authors would like to thank Ms. Xiaohong Zhang for technical assistance.

References

1. Upadhya, K., Yang, J.-M. and Hoffman, W. P., Materials for ultrahigh temperature structural applications. *Am. Ceram. Bull.*, 1997, **58**(12), 51–56.
2. Cutler, R. A., Engineering properties of borides. In *Ceramics and Glasses, Engineering Materials Handbook*, *Vol. 4*, ed. S. J. Schnerder. ASM International, Materials Park, OH, 1991, pp. 787–803.
3. Mroz, C., Zirconium diboride. *Am. Ceram. Bull.*, 1995, **76**(6), 164–165.
4. Wuchina, E., Opeka, M., Causey, S., Buesking, K., Spain, J., Cull, A. *et al.*, Designing for ultra-high temperature applications: the mechanical and thermal properties of HfB_2, HfC_x, HfN_x, and α-Hf(N). *J. Mater. Sci.*, 2004, **39**(19), 5939–5949.
5. Blum, A. and Ivanick, W., Recent developments in the application of transition metal borides. *Power Met. Bull.*, 1956, **7**, 75–78.
6. Zhang, G.-J., Deng, Z.-Y., Kondo, N., Yang, J.-F. and Ohji, T., Reactive hot pressing of ZrB_2–SiC composites. *J. Am. Ceram. Soc.*, 2000, **83**(9), 2330–2332.
7. Levine, S. R., Opila, E. J., Halbig, M. C., Kiser, J. D., Singh, M. and Salem, J. A., Evaluation of ultra-high temperature ceramics for aeropropulsion use. *J. Euro. Ceram. Soc.*, 2002, **22**, 2757–2767.

8. Monteverde, F., Bellosi, A. and Guicciardi, S., Processing and properties of zirconium diboride-based composites. *J. Euro. Ceram. Soc.*, 2002, **22**, 279–288.
9. Chamberlain, A. L., Fahrenholtz, W. G. and Hilmas, G. E., Pressureless sintering of zirconium diboride. *J. Am. Ceram. Soc.*, 2006, **89**(2), 450–456.
10. Tripp, W. C., Davis, H. H. and Graham, H. C., Effect of a silicon carbide addition on the oxidation of zirconium diboride. *Am. Ceram. Bull.*, 1973, **52**(8), 612–616.
11. Chamberlain, A. L., Fahrenholtz, W. G., Hilmas, G. E. and Ellerby, D. T., High-strength zirconium diboride-based ceramics. *J. Am. Ceram. Soc.*, 2004, **87**(6), 1170–1172.
12. Fahrenholtz, W. G., Hilmas, G. E., Chamberlain, A. L. and Zimmermann, J. W., Processing and characterization of ZrB_2-based ultra-high temperature monolithic and fibrous monolithic ceramics. *J. Mater. Sci.*, 2004, **39**(19), 5951–5957.
13. Monteverde, F. and Bellosi, A., Oxidation of ZrB_2-based ceramics in dry air. *J. Electrochem. Soc.*, 2003, **150**(11), B552–B559.
14. Monteverde, F. and Bellosi, A., Development and characterization of metal-diboride-based composites toughened with ultra-fine SiC particulates. *Solid State Sci.*, 2005, **7**, 622–630.
15. Monteverde, F., Beneficial effects of an ultra-fine α-SiC incorporation on the sinterability and mechanical properties of ZrB_2. *Appl. Phys. A: Mater. Sci. Eng.*, 2006, **82**(2), 329–337.
16. Rezaie, A., Fahrenholtz, W. G. and Hilmas, G. E., Effect of hot pressing time and temperature on the microstructure and mechanical properties of ZrB_2–SiC, *J. Mater. Sci.*, in press.
17. Chantikul, P., Anstis, G. R., Lawn, B. R. and Marshall, D. B., Critical evaluation of indentation techniques for measuring fracture toughness: II. Strength method. *J. Am. Ceram. Soc.*, 1981, **64**(9), 539–543.
18. Zhang, S. C., Fahrenholtz, W. G. and Hilmas, G. E., Pressureless densification of zirconium diboride with boron carbide additions. *J. Am. Ceram. Soc.*, 2006, **89**(5), 1544–1550.
19. Telle, R., Sigl, L. S. and Takagi, K., Boride-based hard materials. In *Handbook of Ceramic Hard Materials*, ed. R. Riedel. Wiley-VCH, Weinheim, Germany, 2000, pp. 803–945.
20. Nielsen, L. F., Elasticity and damping of porous materials and impregnated materials. *J. Am. Ceram. Soc.*, 1984, **67**(2), 93–98.
21. Lee, H. and Speyer, R. F., Hardness and fracture toughness of pressureless-sintered boron carbide (B_4C). *J. Am. Ceram. Soc.*, 2002, **85**(5), 1291–1293.
22. Swanson, P. L., Fairbanks, C. L., Lawn, B. R., Mai, Y.-W. and Hockey, B. J., Crack-interface grain bridging as a fracture resistance mechanism in ceramics: I. experimental study on alumina. *J. Am. Ceram. Soc.*, 1987, **70**(4), 279–289.
23. Anne, G., Put, S., Vanmeensel, K., Jiang, D., Vleugels, J. and Biest, O. V., Hard, tough and strong ZrO_2–WC composites from nanosized powders. *J. Euro. Ceram. Soc.*, 2005, **25**, 55–63.
24. Lawn, B., *Fracture of Brittle Solids*. Cambridge University Press, Cambridge, UK, 1993, pp. 30–33.
25. Cook, R. F., Lawn, B. R. and Fairbanks, C. J., Microstructure-strength properties in ceramics: I. Effect of crack size on toughness. *J. Am. Ceram. Soc.*, 1985, **68**(11), 604–615.